

A new approach to identification of transient power quality problems using linear combiners

P.K. Dash ^{a,*}, A.C. Liew ^a, M.M.A. Salama ^a, B.R. Mishra ^b, R.K. Jena ^b

^a *Department of Electrical Engineering, National University of Singapore, 10 Kent Ridge Crescent, Singapore-0511, Singapore*

^b *Department of Electrical Engineering, Regional Engineering College, Rourkela-769 008, Singapore*

Abstract

In this paper, we present a new approach to identify transient power quality disturbances using linear combiners and a fuzzy decision support system. The key idea underlying the approach is to obtain the amplitude and the slope of the peak fundamental component of a voltage waveform using adaptive linear combiners, along with nonlinear least mean squares (LMS) algorithm. Fuzzy logic is then used to identify the class to which the waveform belongs by a set of heuristic rules and an uncertainty index. Detailed digital simulation results involving various types of transient power quality disturbances are presented to prove the ability of the new approach in classifying these disturbances

Keywords: Transient power; Linear combiners; Fuzzy logic

1. Introduction

In recent years, there has been a significant deterioration in the quality of electrical power due to proliferation of nonlinear and power-electronically switched loads in power systems. The poor power quality affects the loads, particularly highly sensitive loads such as computers and microprocessor-based controllers, resulting in malfunctions, instabilities, short lifetime, etc. Poor quality of electric power is normally caused by power line disturbances, such as impulses, notches, momentary interruptions, faults, overvoltages, undervoltages and harmonic distortions, voltage flicker, etc. In order to improve the quality of the delivered power, it is imperative to know the sources and causes of these disturbances and also to classify them.

The process of obtaining power quality data involves the design of the points of measurement, selection of electrical parameters like voltage and current waveforms to be measured, the selection of sensors, the design of instrumentation and cabling and A/D and D/A conversions of data, etc. The power system disturbance waveforms like voltage sag, swell, impulse and

harmonics, voltage flicker, etc. are characterized by certain features, which will be sufficient to distinguish them from the voltage waveform data collected from electrical transmission and distribution systems.

The currently known method for detecting power quality disturbances is based on a point-to-point comparison of adjacent cycles [1]. This method inherently suffers from the drawback that it fails to detect and identify periodic disturbances, such as phase controlled load voltage wave shapes. Past research has considered the applications of neural networks to classification of waveforms due to high and low impedance faults [2–4], magnetizing inrush [5] and power quality issues. In a recent paper [6], the neural network approach was used to identify power system disturbances. This approach seems appropriate to detect and identify a particular type of disturbance; however, due to its intrinsic nature, a specific neural network architecture is required to detect a particular type of disturbance. Thus, the time delay neural network and BP neural network will not be in general able to identify all classes of disturbances.

In this paper, we propose a new approach to detect and localize various types of power quality disturbances, including harmonic distortion using an adaptive linear combiner [7] and a rule-based fuzzy logic decision system [3]. The input to the fuzzy classifier is from a

* Corresponding author..

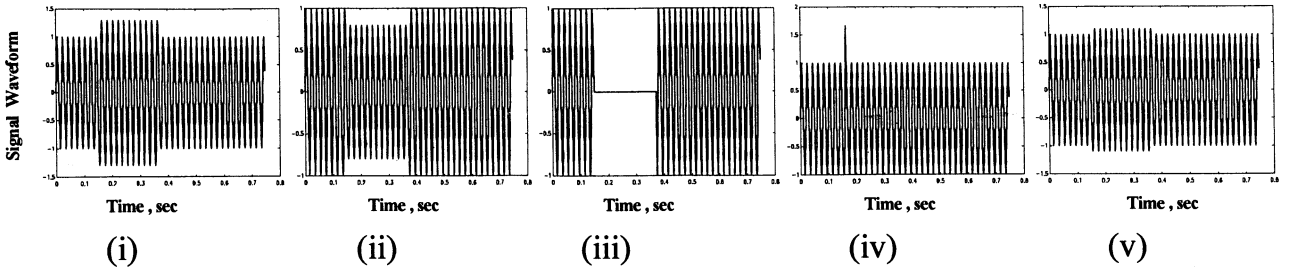


Fig. 1. Different classes of disturbance waveforms showing (i) swell; (ii) sag; (iii) outage; (iv) surge; and (v) distortion.

voltage waveform data preprocessing block known as linear combiners whose weights are adapted by a normalised least mean squares (LMS) algorithm. Several voltage waveforms belonging to the disturbances classes like sag, swell, impulse, outage, harmonic distortion and voltage flicker, etc. are tested using this new approach and in most cases, the event is classified accurately. The identified waveform has the highest credibility or belief factor as defined in the paper in the context of fuzzy classifier.

2. Outline of the method

This section outlines the various power quality disturbance waveforms as described below.

Impulse: waveforms in this class are described as high frequency transients and occur due to capacitor switching, load start-up and lightning, etc.

Voltage sag: the waveforms in this class are characterized by short-term decrease of voltage magnitude and are measured on a cycle-to-cycle basis. System faults and motor startups, etc. cause this kind of voltage problem. The majority of voltage sags have a magnitude around 80% of the normal value and duration of 4–10 cycles.

Harmonic distortion: voltage and current signals become distorted due to harmonic penetration into the

power network and voltage and current total harmonic distortions (THDs) exceed 5% of the magnitude of the fundamental component. This class of disturbance is due to the use of nonlinear loads and adjustable speed drives, etc.

Voltage swell: these waveforms are characterized by short-term increase in the line voltage caused primarily by over-excitation, load unbalancing and capacitive loads.

Outage: an outage is an absence of usable power at some point of the power system and the waveforms that can be characterized as such fall into this class. These are caused by system faults and opening of circuit breakers.

Having chosen the classes of disturbance waveforms as shown in Fig. 1, the next step in the development of a classifier lies in the selection and extraction of desired features of these waveforms. Any successful classification scheme should have a strong noise rejection capability and should be able to handle bad data and frequency excursions. The preprocessor block of the classifier computes the peak amplitude (A) and its change (S) on a sample to sample basis using a normalised least mean squares algorithm (NLMS), as described in Section 3. The inputs to the fuzzy classifier are A and S and an uncertainty index λ_k and the output is the type of waveform and its credibility factor (maximum value is 1). The fuzzy classifier is described in Section 4.

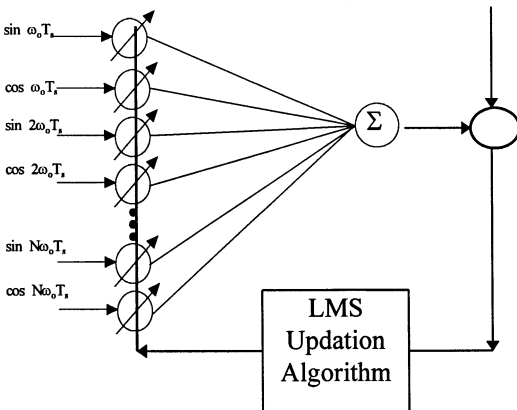


Fig. 2. Block diagram for estimation of fundamental and harmonic amplitudes.

3. Identification of the voltage waveform model

The power system voltage or current waveform is assumed to comprise fundamental and harmonic components as

$$y(t) = \sum_{i=1}^N A_i \sin(i\omega_0 t + \phi_i) \quad (1)$$

where A_i and ϕ_i are the amplitude and phase of the harmonics, N is the total number of harmonics and ω_0 is the angular frequency of the fundamental component of the signal. To obtain the solution for on-line estimation of amplitude of the fundamental component and

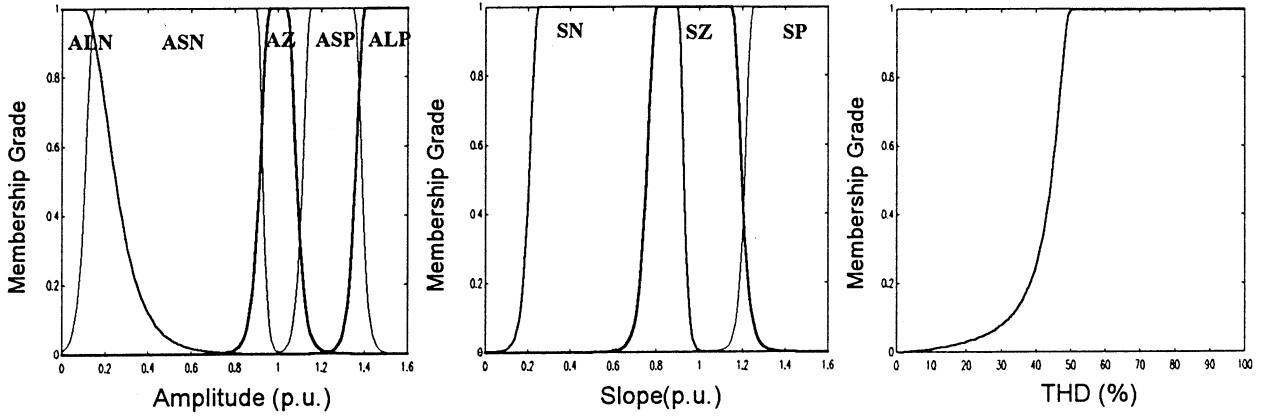


Fig. 3. Membership grades for amplitude, slope and THD.

the total harmonic distortion THD, an adaptive linear combiner along with the nonlinear LMS algorithm is used. The discrete representation of the signal in Eq. (1) is obtained as

$$y(k) = (A_1 \cos \phi) \sin \theta + (A_2 \sin \phi) \cos \theta + \dots + (A_N \cos \phi_N) \sin \theta + (A_N \sin \phi_N) \cos \theta \quad (2)$$

where $\theta = 2\pi k/N_s$, k is the sample number or iteration count and N_s is the sample rate. Eq. (2) is rewritten as

$$y(k) = W^T \psi(k) \quad (3)$$

where

$$y(k) = [A_1 \cos \phi_1 \ A_1 \sin \phi_1 \dots A_N \cos \phi_N \ A_N \sin \phi_N] \quad (4)$$

and

$$\psi^T(k) = [\sin \theta \ \cos \theta \dots \sin \theta_N \ \cos \theta_N]$$

The weight vector of the adaptive linear combiner can be updated using an NMLS algorithm as

$$W(k+1) = W(k) + \frac{\alpha(k)}{L(k)} [y(k) - \psi^T(k)W(k)] \cdot Sgn(\psi(k)) \quad (5)$$

$$L(k) = \lambda + \psi^T(k) \cdot Sgn(\psi(k)) \quad (6)$$

In the above formulation, $\lambda > 0$ and the Sgn function is given by

$$Sgn(x_i) = \begin{cases} +1, & \text{if } x_i > 0 \\ -1, & \text{if } x_i < 0 \end{cases}$$

and

$$Sgn(x_i) = 0, \quad \text{if } x_i = 0 \quad (7)$$

The normalised LMS algorithm used in conjunction with a linear combiner is much superior to the standard Fourier algorithm for the computation of the fundamental component in the presence of harmonics and noise. Both DFT and FFT are prone to errors varying

from 12 to 15% of the actual amplitude in the presence of significant waveform distortion and noise. The convergence of this algorithm has been reported in Dash et al. [8].

Fig. 2 shows the block diagram for the linear combiner. The learning parameter α in the above algorithm controls the convergence and noise rejection property of the algorithm. Using a Lyapunov formalism it can be proven that the value of the parameter lies between $0 < \alpha < 2$ for convergence and noise rejection. It is seen that a small α is required for a periodic sinusoidal waveform and large α is required for a voltage waveform corrupted by noise and distortions. The Lyapunov energy function V is chosen as

$$V(k) = e^2(k) + c_1(\dot{e}(k))^2, \quad c > 0 \quad (8)$$

where

$$e(k) = \text{error} = y(k) - \psi^T(k)W(k) \quad (9)$$

and

$$\dot{e}(k) = (e(k) - e(k-1))/\Delta T \quad (10)$$

where ΔT is the sampling interval. The change in the Lyapunov function $V(k)$ is calculated as

$$\Delta V(k) = V(k) - V(k-1) \quad (11)$$

The learning parameter α is chosen as

$$\alpha(k) = \alpha_0 + c_2 V(k), \quad \text{for } \Delta V(k) > 0 \quad (12)$$

and

$$\alpha(k) = \alpha_0 - c_2 V(k), \quad \text{for } \Delta V(k) < 0 \quad (13)$$

where α_0 is the initial value of the learning parameter and $c_1 > 0$, $c_2 > 0$. The constants c_1 and c_2 are chosen to give suitable weightings to change in the error and change in the Lyapunov energy function. In this paper the values of c_1 and c_2 are chosen as $c_1 = 0.5$ and $c_2 = 0.1$.

The peak amplitude and phase of the fundamental and harmonic components are estimated from the weight vector W as follows:

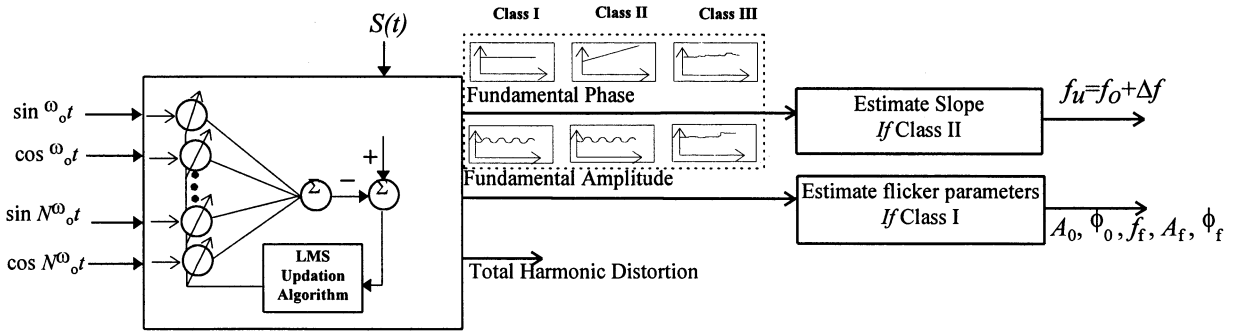


Fig. 4. Determining the waveform class and estimating the dynamic frequency change (Class II).

$$A_i = \sqrt{W_i^2(k) + W_{i+1}^2(k)} \quad (14)$$

and

$$\phi_i = \tan^{-1}(W_{i+1}(k)/W_i(k)) \quad (15)$$

The THD is calculated as

$$\text{THD} = \frac{1}{A_1} \sqrt{\sum_{i=2}^N A_i^2} \quad (16)$$

To obtain the power quality (PQ) index due to harmonic distortion an index is calculated as

$$\lambda_{\text{PQ}} = \frac{P}{\sqrt{\sum_{i=1}^N VI}} \quad (17)$$

The index is an identification of the source side or load side PQ distortion.

4. Classification of disturbance waveforms using fuzzy logic

Fuzzy logic provides an effective method in analysing the highly nonlinear and uncertain data occurring in a power system. To classify the PQ disturbance waveforms, it is preferable to apply a multicriteria decision making approach using fuzzy logic. These methods are neither OR nor AND aggregations, but weighting procedures, taking into consideration the support for a decision from a set of support or truth values. The input parameters used for fuzzification are the peak fundamental component of the voltage signal from a distribution bus of a power system network and its rate of change. The peak amplitude is designated as A and its rate of change is S . The value of S is obtained thus:

$$S(k) = \frac{A(k) - A(k-1)}{\Delta T} \quad (18)$$

For classifying the disturbance waveforms, three fuzzy sets are chosen for the slope as SN (slope negative), SP (slope positive) and SZ (slope zero). In a similar manner, five fuzzy sets are chosen for the peak amplitude A , which are termed ALN (amplitude large

negative), ASN (amplitude small negative), AZ (amplitude zero), ASP (amplitude small positive) and ALP (amplitude large positive). Bell-shaped functions are used to obtain the membership grades for both the amplitude and slope of the waveforms as

$$\mu(x) = \frac{1}{\left(1 + \frac{x - a_1}{c}\right)^{b_1}}, \quad \text{for } x < a_1$$

and

$$\mu(x) = 1, \quad \text{for } a_1 < x < a_2 \quad (19)$$

and

$$\mu(x) = \frac{1}{\left(1 + \frac{x - a_2}{c}\right)^{b_1}}, \quad \text{for } x > a_2 \quad (20)$$

Typical values of a_1, a_2, b_1, b_2 and c for the set ALN are given by

$$a_1 = 0, a_2 = 0.1, b_1 = 2, b_2 = 3, c = 0.1$$

The fuzzy rule base for this pattern classification problem is given below:

Rule 1: IF A is ASP AND S is SP THEN the waveform is Swell.

Rule 2: IF A is ALP AND S is SP THEN the waveform is Surge.

Rule 3: IF A is ASN AND S is SN THEN the waveform is Sag.

Rule 4: IF A is AZ AND S is SZ THEN the waveform is Normal.

Rule 5: IF A is ALN AND S is SN THEN the waveform is Surge.

Rule 6: IF A is ASP AND S is SZ THEN the waveform is Swell.

Rule 7: IF A is ALN AND S is SN THEN the waveform is Surge.

Rule 8: IF A is ALP AND S is SZ THEN the waveform is Sag.

Rule 9: IF A is ALN AND S is SZ the waveform is Outage.

Rule 10: IF A is ALN AND S is SP the waveform is an Outage.

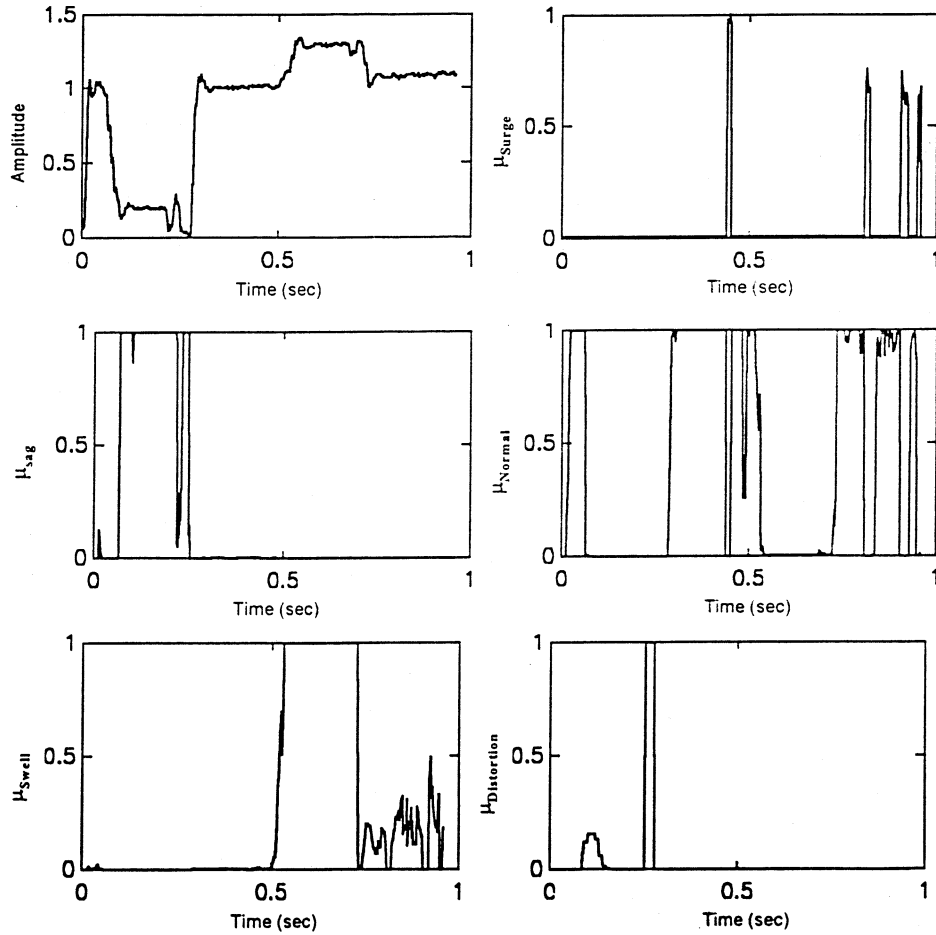


Fig. 8. Output of fuzzy-expert module for the test waveform.

5. Voltage flicker estimation

Voltage flicker in power systems refers to slow 0.5–30 Hz frequency modulation of the voltage waveform. The characteristic of the instantaneous flicker depends upon the nature (type and size) of the load as well as the power supply source to which it is connected. The change of voltage magnitude can occur gradually, as in the case of an arc furnace load or suddenly as in the case of starting of a large induction motor, whereas switching of a capacitor bank or tap changing of a regulation transformer are the cases of source related flickers.

The voltage flicker is modelled as an amplitude modulated waveform, where the modulating signal is a sinusoid of random frequency and random magnitude. The generalized waveform of the voltage signal (the same as Eq. (1), but with a variable amplitude $A_i(t)$) is given by

$$y(t) = \sum_{i=1}^N A_i(t) \sin(i\omega_0 t + \phi_i) + \eta \quad (27)$$

The fundamental component $A_i(t)$ comprises

$$A_1(t) = \{A_{10} + A_{1f} \cos(\omega_f t + \phi_i) + \xi\} \quad (28)$$

where A_{1f} , ω_f and ϕ_i are the amplitude, frequency and phase of the voltage flicker; and η and ξ are the random noise components of zero mean and variance unity, respectively.

The estimation of the voltage flicker parameters will require two steps. In the first step, the fundamental time varying component will be obtained using a linear combiner shown in Fig. 3. In the second step, the time varying component will be passed through a low pass filter (LPF) and two linear combiners to estimate the flicker parameters (shown in Fig. 4).

For the estimation of the component $A_1(k)$ (the discrete version of Eq. (28)), the input vector to the linear combiner is given by

$$y^T(k) = [\cos \omega_0 k T_s \quad \sin \omega_0 k T_s \quad \cos 2\omega_0 k T_s \quad \sin 2\omega_0 k T_s \dots \cos N\omega_0 k T_s \quad \sin N\omega_0 k T_s] \quad (29)$$

where T_s is sampling time.

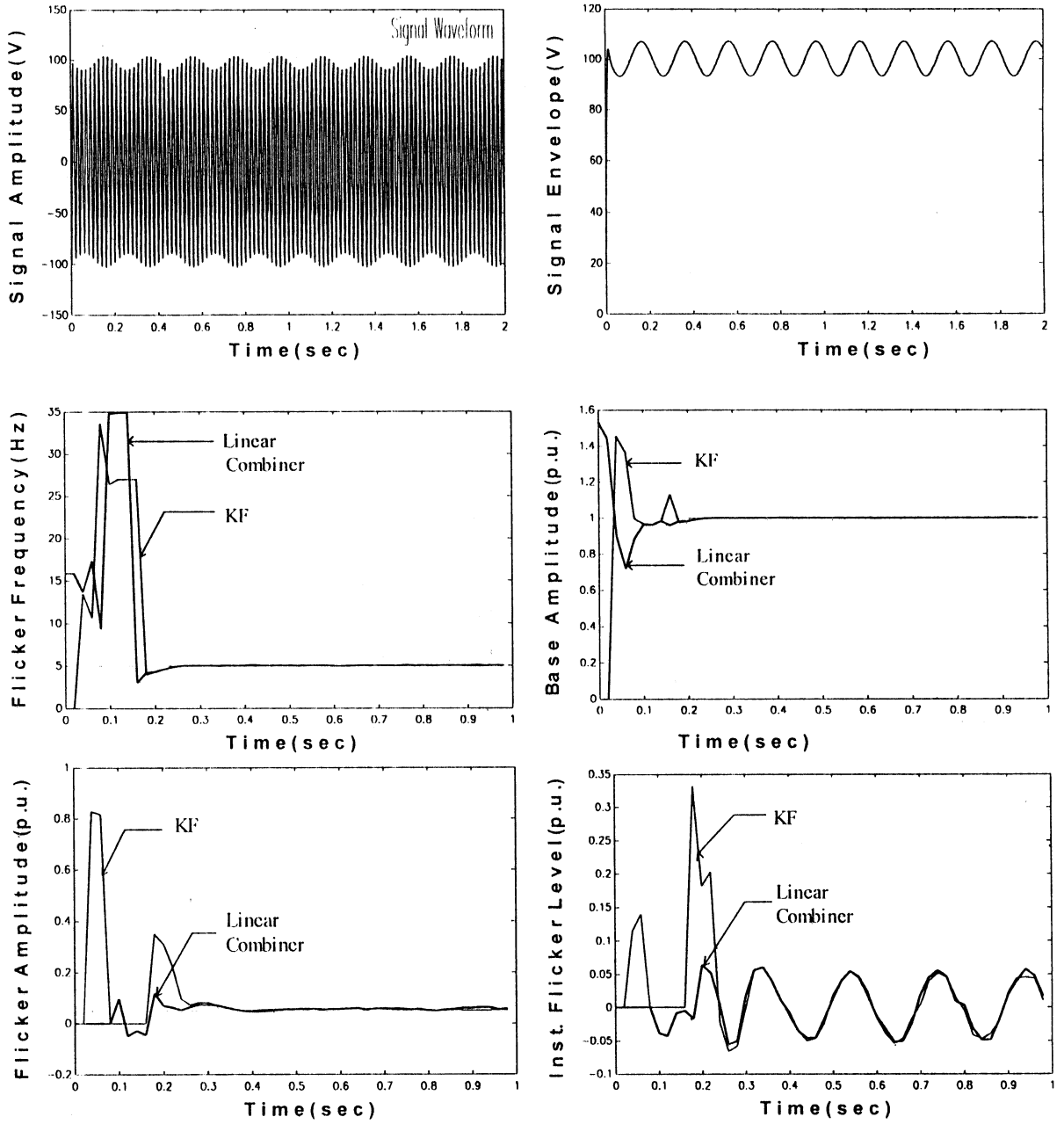


Fig. 9. Estimated flicker parameters.

The weight vector W' adapted as given in Eqs. (5) and (6) to yield $A_1(t)$ and its phase $\phi_1(t)$. As the fundamental amplitude carries the flicker information, we shall denote it as $y_f(k)$, which is equal to the fundamental amplitude $A_1(k)$ at the k th sampling instant.

$$y_f(k) = A_{10} + A_{1f} \cos(\omega_f t + \phi_i) + \delta_k \quad (30)$$

where δ_k is a random sequence that takes into account the noise inherited from the original signal and that introduced by the measurement process. This sequence can prove to be troublesome in estimating the flicker parameters. To reduce the effect of noise, a suitably

designed filter can be used. While selecting the filter order the accuracy must be kept in mind without accounting for unnecessary delay. The filtered signal $y'_f(k)$ is given by

$$y'_f(k) = A_{10} + A_{1f} \cos(\omega_f t + \phi'_i) \quad (31)$$

ϕ'_f will be slightly different from ϕ_i due to phase-shift introduced by the filter.

Using four consecutive samples of the discrete signal given above, this can be shown that

$$\{y'_f(k) - y'_f(k-3)\} - (1 - 2 \cos \omega_f T_s) \{y'_f(k-1) - y'_f(k-2)\} = 0 \quad (32)$$

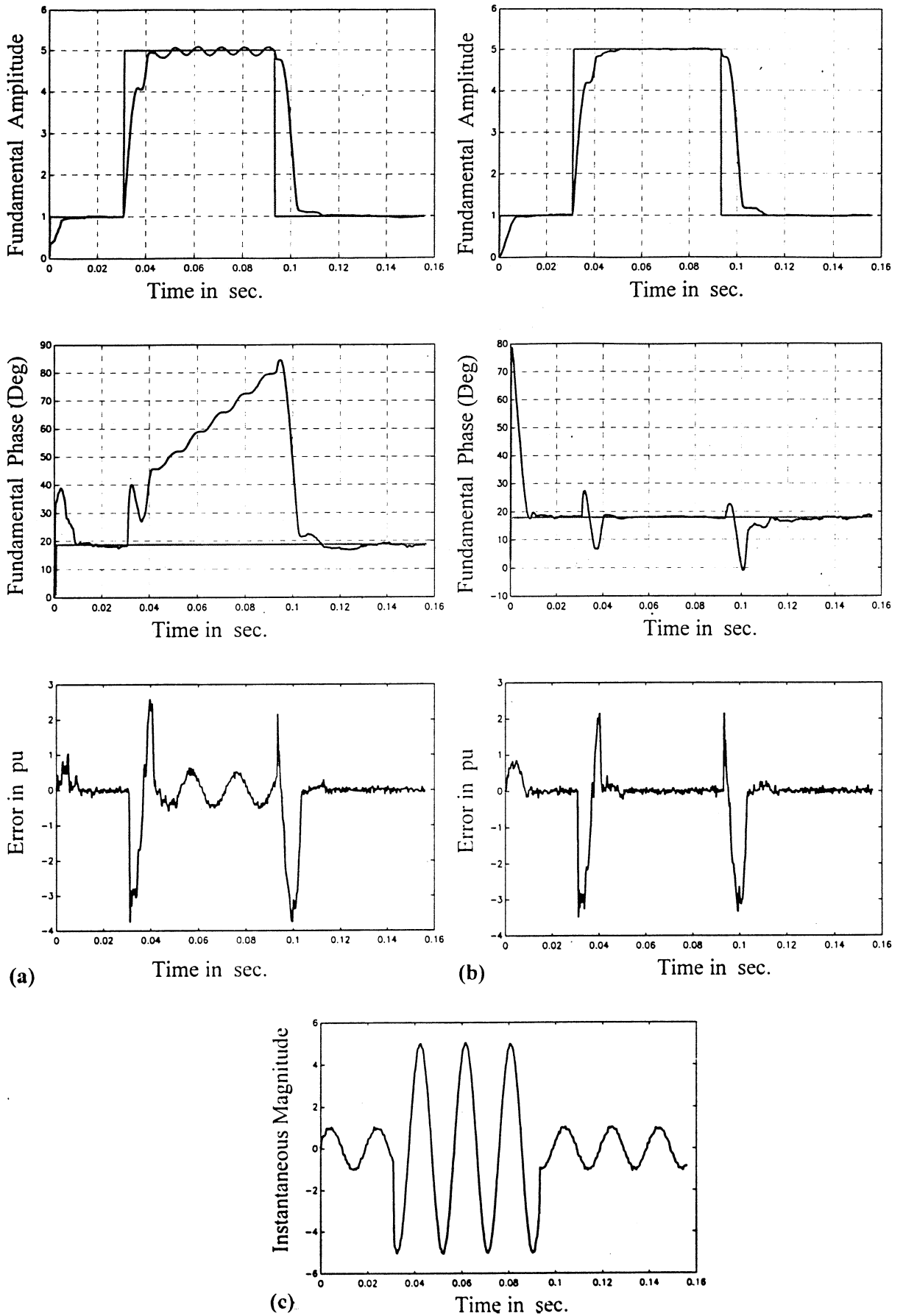


Fig. 10. Effect of frequency change on transient variation of the amplitude of the signal: (a) frequency change unknown; (b) frequency change known; and (c) instantaneous signal wave form.

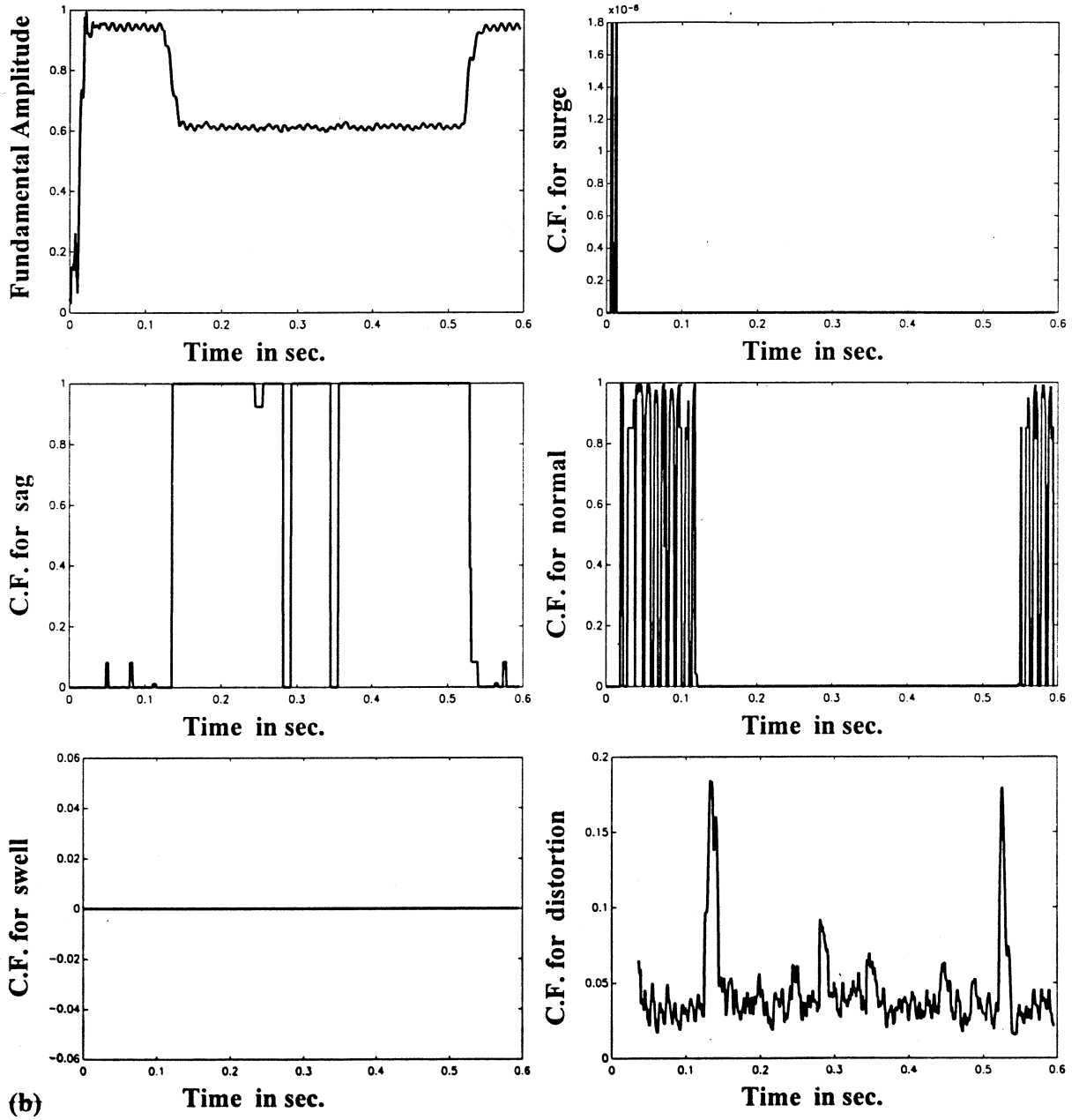
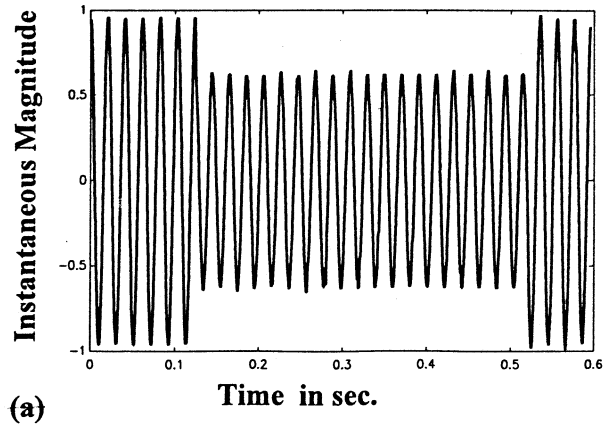


Fig. 11. (a) Phase voltage waveform obtained from the test; (b) confirmation factors of sag, swell and surge in on-line data.

From the above equation, the flicker frequency ω_f can be estimated recursively from the weight vector $W''(k)$ as

$$\omega_f = \frac{1}{T_s} \arccos \left(\frac{W'_2(k)}{W'_1(k)} - 1 \right) \quad (33)$$

Once the flicker frequency is estimated, the base amplitude and flicker amplitude and phase can be found out by another linear combiner as shown in Fig. 3.

The input vector is given by

$$\psi^T(k) = [1 \cos k\omega_f T_s \sin k\omega_f T_s] \quad (34)$$

and A_{10} and A_{1f} are obtained as

$$\begin{aligned} A_{10}(k) &= W''_1(k) \\ A_{1f}(k) &= [\{W''_2(k)\}^2 + \{W''_1(k)\}^2]^{1/2} \end{aligned} \quad (35)$$

It was observed that the flicker estimation becomes ambiguous if there is a mismatch between the system frequency and that assumed in the algorithm for extracting the fundamental envelope, as a frequency drift also produces modulated amplitude pattern. The key to distinguishing between the two events is the fundamental phase, which reveals a positive or negative ramp like response in event of a frequency mismatch. The flicker estimation should completely be inhibited until the frequency mismatch is substantially compensated. To accomplish this, following procedure is adopted:

Compute:

$$\lambda''_k = 2^{-L_k}$$

where the calculations are similar to those of Eqs. (23)–(25), with M_k being modified as

$$M_k = [\phi_1(k)\phi_1(k-1)\dots\phi_1(k+1-N/2)]$$

Rule 11: if λ'_k is LOW and λ''_k is HIGH then Flicker.

Rule 12: if λ'_k is LOW and λ''_k is LOW then Freq. Drift.

6. Results

6.1. Transient disturbances

To test the effectiveness of the proposed new approach, a typical power system shown in Fig. 5 is considered. The power system comprises a short-transmission-line supplying a resistive load (3.3 MW) through a power converter (rectifier). The power system also supplies a constant impedance load and capacitors are placed on the load bus and the converter bus, as shown in the figure, to improve power factor. An EMTDC software package is used to simulate the power system. The initial load current is 18 amps when the power converter is started at $t = 0.043$ s. An outage at the generator end is initiated at $t = 0.49$ s and

persists for 0.04 s. (two cycles based on the 50 Hz supply frequency). Fig. 6 shows the instantaneous converter bus voltage waveform (A-phase only).

A MATLAB software package is used to estimate the amplitude and slope of the simulated bus voltage waveforms. 10% random noise is added (based on the peak amplitude of the fundamental component) to the simulated waveform to provide the waveform patterns, which usually occur in practical situations. Various fuzzy indices are shown in Fig. 7 and the fuzzy index which has the highest membership grade or truth value is chosen to indicate the class of the waveform. For example, during 0.1–0.2 s, $\mu_{\text{Sag}} = 1$, $\mu_{\text{Surge}} = 0$, $\mu_{\text{Swell}} = 0$, $\mu_{\text{Distortion}} = 0$, etc. Thus, during this period a voltage sag has occurred. Similarly, during 0.6–0.7 s, $\mu_d = 0$, μ_{Surge} varies between 0.09 and 0.1, $\mu_{\text{Sag}} = 0$, $\mu_{\text{Swell}} = 0$, and $\mu_{\text{Distortion}} = 0$, thus indicating the presence of Swell.

In the above estimation the linear combiner is started with initial weight vector as a null vector (all the elements are zeros) and the values of α_{max} and α_{min} are kept between 1.2 and 0.6, respectively. Furthermore, it is observed from these simulations that the truth value of a particular category of waveform rises from zero to 100%, if it exists during a particular period. The classification is found to be excellent, even in the presence of noise and harmonic distortions.

6.2. Flicker estimation

Voltage flicker is simulated using the MATLAB software package from the signal represented as

$$\begin{aligned} y(t) &= \{1 + 0.05 \cos(44t + 20^\circ) + \eta_k\} \\ &\{\sin(2\omega_0 t + 60^\circ) + 0.3 \sin(3\omega_0 t + 60^\circ) \\ &+ 0.1 \sin(5\omega_0 t + 60^\circ) + 0.08 \sin(7\omega_0 t + 60^\circ)\} + \epsilon_k \end{aligned}$$

where, η_k and ϵ_k are two different random noise sequences. The values of η_k and ϵ_k are: $\eta_k = 0.02 \text{ rand}(k)$; and $\epsilon_k = 0.05 \text{ rand}(k)$, where $\text{rand}(k)$ has zero mean and unity variance. The initial weight vector is obtained as a null vector with all the elements initialised to zero. The learning parameter α is updated using a Lyapunov approach, where the constants α_0 , c_1 and c_2 are chosen as $\alpha_0 = 1.2$, $c_1 = 0.5$ and $c_2 = 0$.

The added noise amplitude in this example is nearly 15% of the peak amplitude of the fundamental component (base amplitude). The flicker parameters such as amplitude (A_{1f}), frequency (ω_f) and phase (ϕ_f) are shown in Fig. 8. The signal waveform and its envelope are shown to indicate the presence of a flicker. The estimated values of the above parameters using a 3-stage Kalman filter [5] are also shown in the figure. The envelope of the fundamental frequency component is separated into a constant and time varying component. An extended Kalman filter approach is used to compute the magnitude and frequency of the instantaneous

flicker level. The Kalman gain is computed using suitable noise covariance matrices \mathbf{Q} and \mathbf{R} for providing optimized performance. The \mathbf{Q} and \mathbf{R} matrices are chosen as $\mathbf{Q} = \text{diag}(0.0001)$, $\mathbf{R} = \text{diag}(0.00001)$, respectively. From Fig. 8, it is observed that the proposed approach performs satisfactorily in comparison to the Kalman filter, where the computational overhead is very high in the presence of noise and harmonics.

6.3. Effect of frequency changes on the estimated waveforms

The estimation of amplitude and phase angles of signals corrupted with noise depends on the assumption that the signal frequency is known a priori. However, if the frequency also changes during a transient process, the estimation of fundamental frequency is required for the estimation of signal parameters. A small frequency drift of +2 Hz was initiated at $t = 0.03$ s, accompanied by a sudden change in per unit voltage magnitude. Fig. 9 shows the tracked amplitude and phase of the voltage signal corrupted with a random noise of variance $\sigma = 0.05$.

6.4. Test with real-time data

With a view to real-time application of the proposed approach, data is obtained from a laboratory setup comprising a 230 volt, 50 Hz, 3-phase AC system supplying a balanced R-L load. The system data is acquired through a PCL-7/8 data acquisition card using a 12-bit A/D converter. The data acquisition card has a powerful and easy to use software routine started in the EPROM. A personal computer PC-486, 100 MHz processor is used to process the voltage and current samples using a software program developed in C++ programming language. The proposed algorithm with an adaptive learning parameter α provides fast tracking of the fundamental component of the transient voltage signal, as shown in Fig. 10(a). Fig. 10(b) shows the variation in the amplitude of the fundamental component of the load voltage along with confirmation factors (CF) which are obtained from the fuzzy classifier (Fig. 11). These factors clearly indicate the occurrence of a particular transient disturbance.

7. Conclusions

This paper presents a new approach for monitoring the transient PQ disturbances including voltage flicker. The transient power-line disturbances such as voltage sag, swell, surge, outage, etc. are classified very accurately with the least computational overhead in comparison to neural networks and wavelet transforms. In the case of neural networks, the classification is not found to be robust and significant accuracy is not achieved. The adaptive linear combiners filter noise very effectively and hence produce an accurate classification of transient PQ disturbance waveforms. Voltage flicker parameters due to frequency modulation of the power supply system waveform are also estimated using adaptive linear combiners. The accuracy of this approach and its simplicity outweigh the efficacy of the Kalman filtering approach in estimating the amplitude, frequency and phase of the voltage flicker.

References

- [1] A. McEachern, Handbook of Power Signatures. Basic Measuring Instruments, Foster City, CA, 1988.
- [2] C.J. Kim, B.D. Russell, Classification of faults and switching events by inductive reasoning and expert system methodology, IEEE Trans. Power Deliv. 4 (3) (1989) 1631–1637.
- [3] S. Ebron, D. Lubkeman, M. White, A neural network approach to the detection of incipient faults on power distribution feeders, IEEE Trans. Power Deliv. 5 (2) (1990) 905–914.
- [4] A.F. Sultan, G.W. Swift, D.J. Fedirchu, Detection of high impedance arcing faults using a multilayered perceptron, IEEE Trans. Power Deliv. 7 (4) (1992) 1871–1877.
- [5] L.G. Percz, A.J. Flechsig, J.L. Meador, Z. Obradovic, Training an artificial neural network to discriminate between magnetizing inrush and internal faults, IEEE Winter Power Meeting, 1993, Paper no. WM037-2 PWRD.
- [6] A.K. Ghose, D. Lubkeman, The classification of power system disturbance waveforms using a neural network approach, IEEE Trans. Power Deliv. 10 (1) (1995) 109–115.
- [7] P.K. Dash, A.C. Liew, S. Rahman, Fuzzy neural network and fuzzy expert system for load forecasting, Proc. IEE (London) Gener. Transm. Distrib. 143 (1) (1996) 106–115.
- [8] P.K. Dash, D.P. Swain, A.C. Liew, S. Rahman, An adaptive linear combiner for on-line tracking of power system harmonics, IEEE Trans. Power Syst. 96 WM 181-8 PWRD, January, 1996, pp. 21–25.